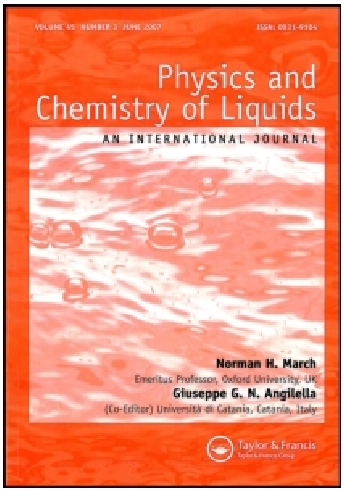

Physics and Chemistry of Liquids
Publication details, including instructions for authors and subscription information:
http://www.informaworld.com/smpp/title~content=t713646857

Non-relativistic and relativistic electron liquids confined by a linear potential

N. H. March[a]; L. M. Nieto[b]
[a] Department of Physics, University of Antwerp (RUCA), Antwerpen, Belgium [b] Departamento de Física Teórica,Atómica y Óptica, Universidad de Valladolid, 47005 Valladolid, Spain

To cite this Article March, N. H. and Nieto, L. M.(2005) 'Non-relativistic and relativistic electron liquids confined by a linear potential', Physics and Chemistry of Liquids, 43: 3, 225 — 237
To link to this Article: DOI: 10.1080/00319100500040963
URL: http://dx.doi.org/10.1080/00319100500040963

Physics and Chemistry of Liquids
Vol. 43, No. 3, June 2005, 225–237

Taylor & Francis
Taylor & Francis Group

Non-relativistic and relativistic electron liquids confined by a linear potential

N.H. MARCH† and L.M. NIETO‡*

†Department of Physics, University of Antwerp (RUCA), 171 Groenenborgerlaan, B–2020, Antwerpen, Belgium and Oxford University, Oxford, England
‡Departamento de Física Teórica, Atómica y Óptica, Universidad de Valladolid, 47005 Valladolid, Spain

(*Received 20 December 2004*)

The theory of fermion particle densities in a confining linear scalar potential energy $V(x) = g|x|$ is considered in both non-relativistic and relativistic quantum mechanics. In the former case, some analytic progress proves possible for weak potentials (small g), by consideration of the canonical density matrix, having the Slater sum as its diagonal element. For larger values of g, some numerical results for the fermion density $\varrho(x)$ are presented, from essentially the properties of Airy functions.

The influence of a non-zero value of the Compton wavelength $\lambda = h/m_0c$, with m_0 the fermion rest mass, is then considered using relativistic Thomas–Fermi theory. For future work, the treatment of Hiller from the Dirac equation should prove amenable to numerical computation of the relativistic fermion density $\varrho_\lambda(x)$, for comparison with the Thomas–Fermi results presented here. The possibility of relativistic and non-relativistic densities being related by a difference equation with an interval determined by λ is briefly referred to.

Keywords: Electron liquids; Canonical density matrix; Slater sum; Relativistic density

PACS: 05.30.Fk; 71.10.Ca; 31.15.Ew; 31.15.Bs

1. Introduction

Current interest in density functional theory spans both non-relativistic and relativistic quantum mechanics. Especially important in the latter area would be the possibility of working with a scalar fermion particle density, rather than with a Dirac spinor in wave function theory. This was emphasized, for example, in the study by Holas and March [1], other references being cited there.

We tackle here a model problem of one-dimensional motion in a linear scalar potential $V(x)$, namely

$$V(x) = g|x| \tag{1}$$

*Corresponding author. E-mail: luismi@metodos.fam.cie.uva.es

Physics and Chemistry of Liquids
ISSN 0031-9104 print: ISSN 1029-0451 online © 2005 Taylor & Francis Group Ltd
DOI: 10.1080/00319100500040963

Our main concern will be to construct the fermion particle density, denoted by $\varrho(x)$, and given in non-relativistic quantum mechanics by

$$\varrho(x) = \sum_{\text{occupied } i} \psi_i(x)\,\psi_i^*(x) \tag{2}$$

For the potential (1), the Schrödinger eigenfunctions $\psi_i(x)$ (in equation (2)) involve Airy functions, the corresponding eigenvalues ϵ_i requiring knowledge of the nodes of these functions (see section 3).

The interest we pursue here is, for the admittedly simple potential (1) which has, however, interest for hadron physics and quark confinement, in addition to electron liquids, to emphasize the question raised earlier [2], as to the relation, say, of $\varrho(x)$ in equation (2) to the relativistic density, denoted throughout by $\varrho_\lambda(x)$, for the same $V(x)$, where λ is the Compton wavelength $\lambda = h/m_0c$. For the potential (1), this is achieved largely by numerical procedures, though some limited analytical results are presented for the non-relativistic limit $c \to \infty$ corresponding to the limit $\lambda \to 0$.

The outline of the present article is as follows. In section 2, we report some analytical results pertaining to the canonical density matrix $C(x, x_0, \beta)$, defined by

$$C(x, x_0, \beta) = \sum_{\text{all } i} \exp(-\beta\epsilon_i)\psi_i(x)\,\psi_i^*(x_0), \quad \beta = (k_\text{B}T)^{-1} \tag{3}$$

where k_B is Boltzmann's constant. We note that $C(x, x_0, \beta)$ is related to the Feynman propagator $K(x, x_0, t)$ through the transformation $\beta \to it$. This matrix satisfies the Bloch equation

$$\mathcal{H}_x\, C(x, x_0, \beta) = -\frac{\partial C(x, x_0, \beta)}{\partial \beta} \tag{4}$$

where $\mathcal{H}_x$ is the one-body Hamiltonian

$$\mathcal{H}_x = -\frac{1}{2}\frac{\partial^2}{\partial x^2} + V(x) \tag{5}$$

The completeness condition of the eigenfunctions $\psi_i(x)$ gives the 'initial' condition under which equation (4) is to be solved as

$$C(x, x_0, \beta = 0) = \delta(x - x_0) \tag{6}$$

In particular, in section 2, some results for the effective potential matrix $U(x, x_0, \beta)$ defined by

$$C(x, x_0, \beta) = C_0 \exp(-\beta\, U(x, x_0, \beta)) \tag{7}$$

where C_0 is the free fermion limit, will be presented, for small values of g in equation (1), the result for U being given correctly up to and including $O(g^2)$. Then in section 3, numerical results will be presented for $\varrho(x)$ in equation (2) using Airy functions, for a variety of occupied energy levels, or equivalently numbers N of fermions. Using eigenfunctions and eigenvalues thereby obtained, some numerical results are also given for the so-called Slater sum $S(x, \beta)$ which is simply the diagonal element $C(x, x, \beta)$ of equation (3).

In section 4, we turn to the relativistic density $\varrho_\lambda(x)$, as given by relativistic Thomas–Fermi theory [3]. Section 5 then makes a start on the problem referred to above of relating $\varrho(x)$ and $\varrho_\lambda(x)$ for this model potential (1). Finally, section 6 constitutes a summary plus some proposals for further study which may prove fruitful.

2. Canonical density matrix for potential $V(x) = g|x|$ for g small

To get analytical results for the canonical density matrix, we have used the perturbation theory of March and Stoddart [4] for the effective potential matrix $U(x, x_0, \beta)$ defined in equation (7). This satisfies, to first order in $V(x)$, the equation

$$U_1(x, x_0, \beta) = \int_{-\infty}^{\infty} dx_1 \int_0^1 da\, C_0(x_1 - x_0, a(x - x_0), a(1-a)\beta)\, V(x_1) \tag{8}$$

Here, the explicit form of the free fermion matrix $C_0(x, x_0, \beta)$ was already known to Sondheimer and Wilson [5], and is given by

$$C_0(x, x_0, \beta) = \frac{1}{\sqrt{2\pi\beta}} \exp\left(-\frac{(x - x_0)^2}{2\beta}\right) \tag{9}$$

By gradient expansion of $V(x_1)$, the result of March and Stoddart [4, therein equation (A 2.2)], for the linear potential (1) reduces to the form

$$U_1(x, x_0, \beta) = \int_0^1 da\, V(ax + (1-a)x_0) \tag{10}$$

which clearly yields, on the diagonal $x_0 = x$, the intuitively simple result

$$U_1(x, x, \beta) = V(x) \tag{11}$$

However, for x_0 not equal to x, the potential $V(x) = g|x|$ needs careful consideration, requiring treatment of different regimes of x and x_0. The final result in compact form is given by

$$U_1(x, x_0, \beta) = \frac{g}{2(x - x_0)} \left(x|x| - x_0|x_0|\right) \tag{12}$$

As March and Stoddart also note, though they do not consider potential (1), in their equation (A 2.6), there is a term to be added at $O(g^2)$: denoted by U_2 below and given by

$$U_2(x, x_0, \beta) = \frac{\beta^2}{6} \left\{ \int_0^1 da\, \frac{\partial}{\partial x} V(ax + (1-a)x_0) \right\}^2 \tag{13}$$

In the case of an odd potential $V = gx$, this result is readily evaluated to yield $U_2 = (\beta^2 g^3)/24$, and with U_1 as in equation (11) one has the exact Slater sum of this odd potential. However (see also figure 6 later in this article), for the even potential $V = g|x|$,

U_2 has a singular form as $x_0 \to x$, $U_2(x,x_0,\beta)=(\beta^2 g^2)/(12(x-x_0)^4)(|x|(x-x_0)+x_0(|x|-|x_0|))$, showing, in contrast to figure 6, that truncating gradient expansions fail in this case.

Having constructed these analytical results for the $C(x, x_0, \beta)$ matrix for small g, we turn immediately to obtain the corresponding fermion densities $\varrho(x)$ from equation (2), for fermion numbers N, but now for large g.

3. Particle density and kinetic energy density as function of number N of fermion levels occupied

The Airy functions are denoted by Ai(x): our aim in this section is to display first the fermion particle density $\varrho_N(x)$ defined by (see also Hiller [6], who however, was concerned with wave functions and eigenvalues, not $\varrho(x)$)

$$\varrho_N(x) = \sum_{i=1}^{N} \Big[N_i \, \mathrm{Ai}(|x| - 2\epsilon_i) \Big]^2 \tag{14}$$

where the ϵ_i denote the zeros of Ai(x) and Ai$'(x)$:

$$\mathrm{Ai}'(-2\epsilon_n) = 0 \longrightarrow \epsilon_1, \epsilon_3, \epsilon_5, \ldots \tag{15}$$

and

$$\mathrm{Ai}(-2\epsilon_m) = 0 \longrightarrow \epsilon_2, \epsilon_4, \epsilon_6, \ldots \tag{16}$$

The results for the nodes in equations (15) and (16) are displayed in table 1, together with the lowest 20 adimensional eigenvalues ϵ_i. (The eigenenergies depend on the physical parameters and are indeed given by $E_i = ((\hbar^2 g^2)/2m)^{1/3} \epsilon_i$.)

Table 1. Low-lying eigenvalues ϵ_i for linear scalar potential $V(x) = g|x|$.

	Zeros of Ai(x)	Zeros of Ai$'(x)$	ϵ_i
1		−1.01879	1.01879
2	−2.33811		2.33811
3		−3.24820	3.24820
4	−4.08795		4.08795
5		−4.82010	4.82010
6	−5.52056		5.52056
7		−6.16331	6.16331
8	−6.78671		6.78671
9		−7.37218	7.37218
10	−7.94413		7.94413
11		−8.48849	8.48849
12	−9.02265		9.02265
13		−9.53545	9.53545
14	−10.04017		10.04017
15		−10.52766	10.52766
16	−11.00852		11.00852
17		−11.47506	11.47506
18	−11.93602		11.93602
19		−12.38479	12.38479
20	−12.82878		12.82878

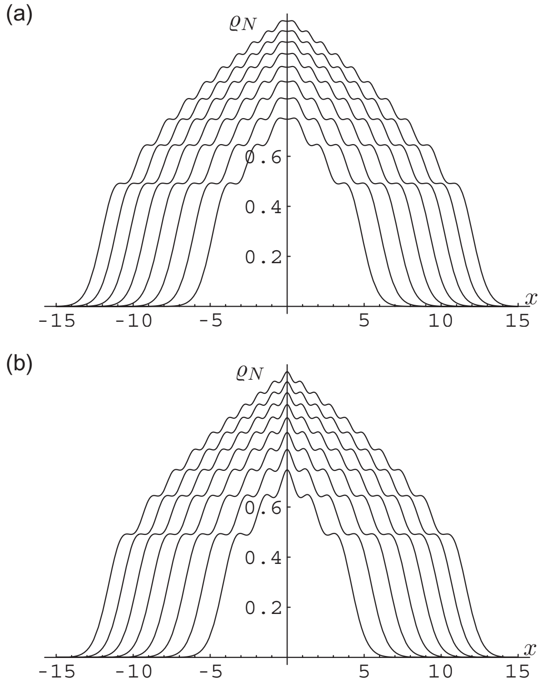

Figure 1. Non-relativistic Fermion particle density ϱ_N: (a) for $N = 6, 8, \ldots, 20$, (b) for $N = 5, 7, \ldots, 19$.

In equation (14), N_i denotes the normalization factor ensuring that there is a single fermion in each occupied level, and hence that

$$\int_{-\infty}^{\infty} \varrho_N(x)\, dx = N \tag{17}$$

The particle densities $\varrho_N(x)$ thereby obtained are displayed in figure 1 for N from 5 to 20, even values being shown on the left of this figure. What is clear is that the features shown as N are varied, remain at constant values of ϱ, the lowest feature being at or near $\varrho = 0.5$, independent of N. Naturally, a new feature appears as each additional level is filled, the spacing in ϱ reducing with increasing N. It is clear from figure 1 that $\varrho_N(0)$ is not (quite!) the maximum of each curve, due to the 'oscillations' in evidence for each value of N shown. Since $\varrho_N(0)$ is a characteristic feature of the fermion density, values of $\varrho_N(0)/N^{1/3}$, an approximately constant quantity ~ 0.424, are given in table 2. That odd and even values of N approach a limiting large N value in a different manner is demonstrated in figure 2.

3.1. *Relation of kinetic energy density to particle density*

The positive definite kinetic energy per unit length, referred to for convenience as kinetic energy density, will be defined by

$$t_g(x) = \frac{1}{2} \sum_{\text{occupied } i} \{\psi_i'(x)\}^2 \tag{18}$$

Table 2. Fermion particle density $\varrho_N(x)$ at the origin, from $N = 6$ to 20. Approximate scaling with $N^{1/3}$ is evident.

N	$N^{1/3}$	$\varrho_N(0)/N^{1/3}$
6	1.81712	0.41188
7	1.91293	0.43366
8	2.00000	0.41478
9	2.08008	0.43142
10	2.15443	0.41653
11	2.22398	0.42999
12	2.28943	0.41770
13	2.35133	0.42900
14	2.41014	0.41854
15	2.46621	0.42828
16	2.51984	0.41916
17	2.57128	0.42772
18	2.62074	0.41965
19	2.66840	0.42728
20	2.71442	0.42004

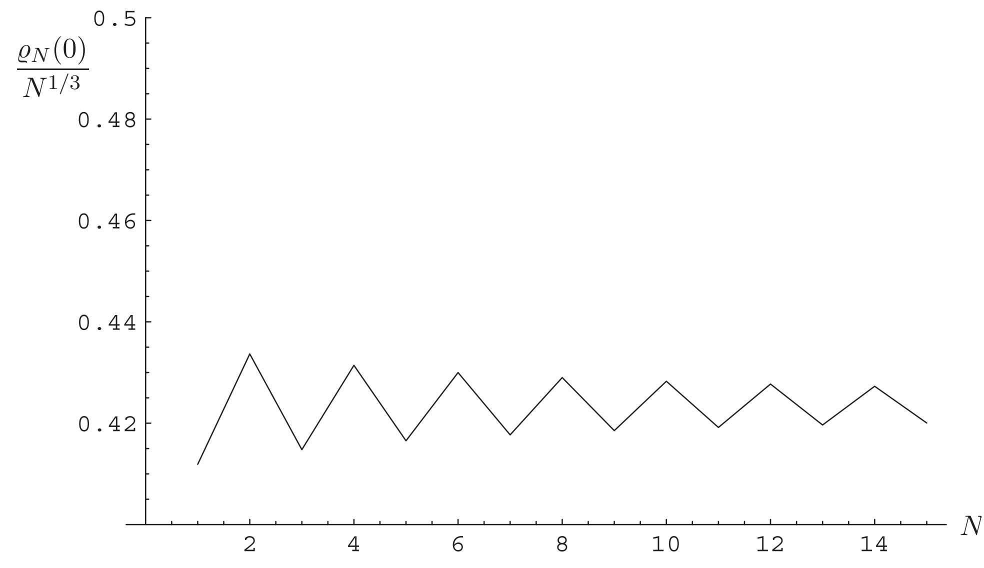

Figure 2. Different behavior of non-relativistic fermion density at the origin for even and odd N, related to Table 2.

Using the Airy functions set out earlier for $\psi_i(x)$, $t_g^N(x)$ is plotted in figure 3, again for N from 5 to 20 inclusive. In the region of tunnelling tails of the wave functions, we show in figure 4(b) the von Weizsäcker [7] inhomogeneity kinetic energy density $t_W(x)$ defined by

$$t_W(x) = \frac{1}{8}\frac{[\varrho'(x)]^2}{\varrho(x)} \tag{19}$$

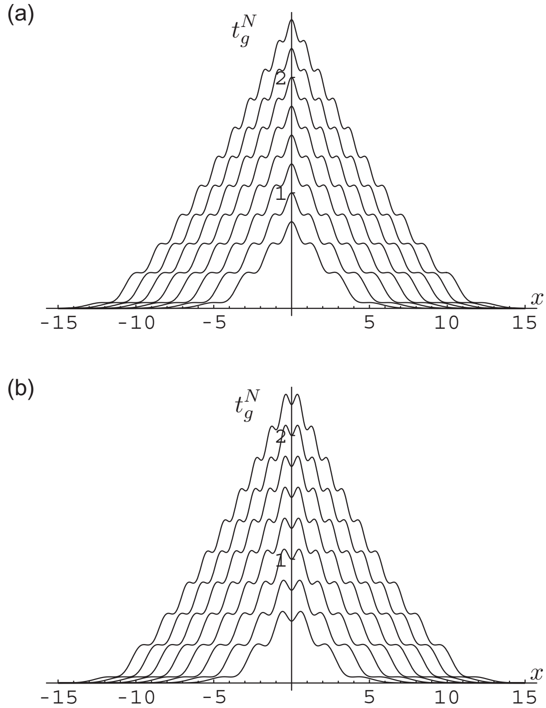

Figure 3. Non-relativistic kinetic energy density t_g^N: (a) for $N = 6, 8, \ldots, 20$, (b) for $N = 5, 7, \ldots, 19$.

for comparison. The kinetic energy density in the tunnelling tails is evidently dominated by the von Weizsäcker form, which has relatively small amplitude elsewhere when $N = 20$.

To complete this section, we provide a link with the canonical density matrix $C(x, x_0, \beta)$ discussed previously, and in particular its diagonal element $C(x, x, \beta)$ which is the Slater sum $S(x, \beta)$, as mentioned earlier. Here, using the wave functions described earlier in terms of Airy functions, plus the corresponding eigenvalues recorded in table 1 (they extend the results given by Hiller [6] up to $N = 20$), we have constructed the 'partial Slater sum' $S_N(x, \beta)$ defined by

$$S_N(x, \beta) = \sum_{i=1}^{N} \exp(-\beta\epsilon_i)\Big[N_i \,\mathrm{Ai}(|x| - 2\epsilon_i)\Big]^2, \tag{20}$$

again for $N = 6$–20. The results for $S_N(x, \beta)$ for $\beta = 1$ and $\beta = 5$ are displayed in figure 5. For comparison, the result $S^1(x, \beta) = (2\pi\beta)^{-1/2} \exp(-\beta\, U_1(x, x, \beta))$ is also shown, with U_1 defined in equation (8). When the diagonal form (equation (11)) is inserted, $S^1(x, \beta)$ becomes, in fact, the Thomas–Fermi approximation to the Slater sum. This is also shown for comparison with the finite sums in figure 5, for again $\beta = 1$ and $\beta = 5$. Except for the non-analytic behavior of $S^1(x, \beta)$ at $x = 0$, the agreement with the finite sum in equation (20) for $N = 20$ is already quite reasonable for $\beta = 1$. However, the Thomas–Fermi result is a small β approximation, and fails for $\beta = 5$ (see figure 5(b)).

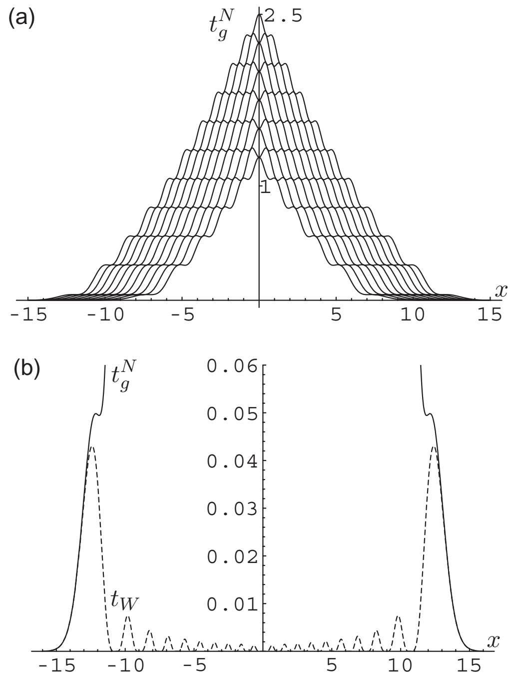

Figure 4. (a) Kinetic energy density t_g^N for $N = 10, 11, 12, \ldots, 20$, (b) Solid line t_g^N, dashed line t_W defined in equation (19), both for $N = 20$.

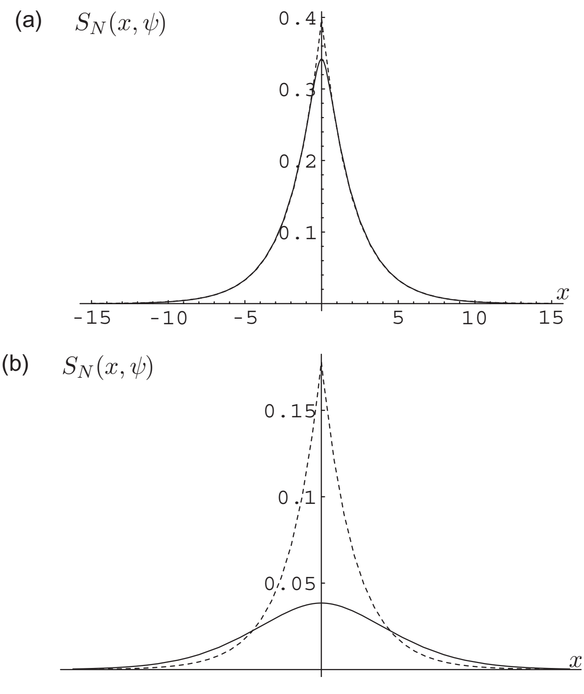

Figure 5. Partial Slater sum $S_N(x, \beta)$, (a) for $\beta = 1$, (b) for $\beta = 5$. The Thomas–Fermi approximation is shown by the dashed lines. It is a small β result, and fails therefore for $\beta = 5$.

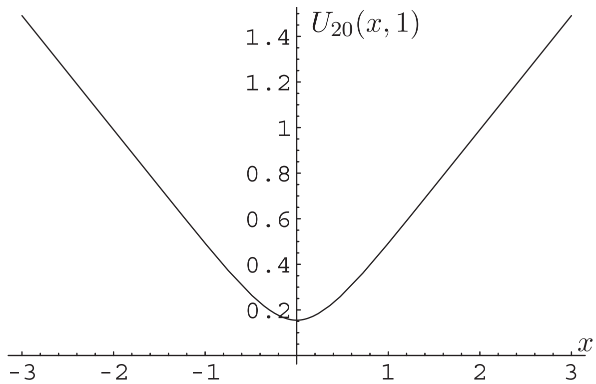

Figure 6. Effective potential matrix $U_{20}(x, \beta = 1)$ from $S_{20}(x, \beta = 1)$, $g = 1/2$ (see equation (20)).

To conclude this section, we have utilized the results for $S_N(x, \beta)$ for $\beta = 1$ and $N = 20$ to construct figure 6, which shows $U(x, \beta)$ thereby extracted from equation (7) with x_0 put equal to x. Deviations from the potential $V(x) = g|x|$ occur only very close to $x = 0$ and validate the equation (11) elsewhere.

4. Relativistic generalization of Thomas–Fermi particle density

The purpose of this section is to effect the relativistic generalization of the fermion particle density exhibited in figure 1 at the level of the Thomas–Fermi approximation.

For the relativistic Thomas–Fermi theory [8], the fermion particle density is given by

$$\varrho_\lambda(x) = \frac{1}{\pi}\sqrt{(\mu_\lambda + m_0 - g|x|)^2 - m_0^2} \tag{21}$$

for $x \in [-x_c, x_c]$, where x_c is a cut-off radius, which in our case takes the value $x_c = \mu_\lambda / g$, μ_λ being the relativistic chemical potential, whose value is obtained from the condition

$$N = \int_{-x_c}^{x_c} \varrho_\lambda(x)\, dx \tag{22}$$

From equations (21) and (22) we obtain an implicit expression for μ_λ as a function of N, g and m_0:

$$(1 + a)\sqrt{a(2 + a)} - 2\,\mathrm{arcsinh}\sqrt{\frac{a}{2}} = \frac{g\pi N}{m_0^2}, \quad a = \frac{\mu_\lambda}{m_0} \tag{23}$$

This quantity $a = \mu_\lambda / m_0$ is plotted versus $g\pi N / m_0^2$ in figure 7.

Inserting $\mu_\lambda(N)$ into equation (21) enables the relativistic Thomas–Fermi density to be calculated. The results are shown in figure 8, where, because the relativistic Thomas–Fermi theory has statistical foundations, it comes into its own at really large values of N. Therefore, in figure 8, we have included plots for N up to 100.

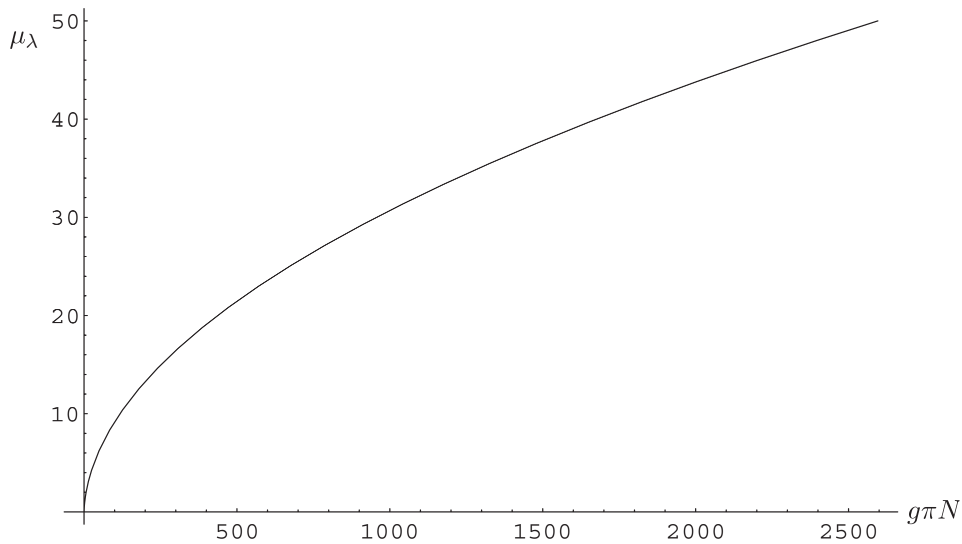

Figure 7. Chemical potential μ_λ as a function of N, with $m_0 = 1$.

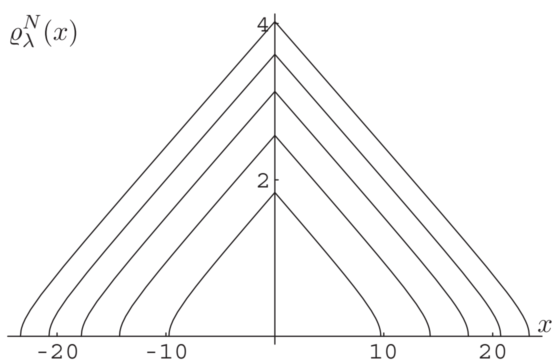

Figure 8. $\varrho_\lambda^N(x)$ for relativistic Thomas–Fermi theory (see equations (21) and (23)), for $N = 20, 40, 60, 80, 100$. Notice the classically forbidden radii in this theory.

5. Can $\varrho_\lambda(x+\delta)$ be directly related to $\varrho(x)$ for an appropriate choice of 'difference' δ, assumed related to the Compton wavelength h/m_0c?

The purpose of this article is to question, given that both relativistic and non-relativistic fermion densities $\varrho_\lambda(x)$ and $\varrho(x)$ are characterized by the same linear potential $V(x) = g|x|$, whether $\varrho_\lambda(x)$ can be related to $\varrho(x)$ in practice. This question was answered in the affirmative by one of us [2], in an earlier work in which both $\varrho_\lambda(x)$ and $\varrho(x)$ were approximated by the Thomas–Fermi theory, valid for large numbers of fermions. Howard and March [9] also proposed an affirmative answer to this question recently, transcending the Thomas–Fermi limit, but now specifically for harmonic confinement in d dimensions. These authors wrote, in the example $d=1$:

$$\varrho_\lambda(x+\delta) = b(x,\delta)\ \varrho(x) \tag{24}$$

where the interval δ was asserted, as above, to be determined by the Compton wavelength. Their heuristic arguments suggested, however, that δ would also depend on the number N of occupied fermion levels. We return briefly to these issues in section 6.

6. Summary and proposed future directions

The main achievements of this study are as follows:

- (i) Approximate forms of the Feynman propagator $K(x, x_0, t)$ or equivalently the canonical density matrix $C(x, x_0, \beta)$ for the non-relativistic theory of the linear potential $V(x) = g|x|$, in section 2.
- (ii) Quantum mechanical fermion particle densities $\varrho(x)$ and kinetic energy densities for non-relativistic fermions, shown in figures 1 and 2, respectively, for numbers of occupied fermion levels N ranging from 5 to 20.
- (iii) Determination of the chemical potential and the fermion density $\varrho_\lambda(x)$ using relativistic Thomas–Fermi theory in figures 7 and 8, respectively.
- (iv) Brief discussion of the possible relation between a 'shifted' relativistic density $\varrho_\lambda(x+\delta)$ and its non-relativistic limit $\varrho(x)$, the interval δ involving the Compton wavelength.

As for future directions, it would of course be important if a third-order linear homogeneous differential equation could be established for $\varrho(x)$, for an arbitrary number N of filled levels, as was done by Lawes and March [10] for harmonic confinement (see also the Appendix). If this further step eventually proves possible, it would then be of interest to extend the heuristic proposal of Howard and March [9] made for harmonic confinement: namely to replace the non-relativistic differential equation by its central difference counterpart, with interval δ (see equation (24)) involving the Compton wavelength. It would, of course, be of considerable interest for future relativistic density functional theory to compare the Dirac density $\varrho_\lambda(x)$ calculated from the work of Hiller [6] with the solution of the resulting difference equation, for various choices of the number of occupied fermion levels. By construction, this procedure would reduce correctly to the non-relativistic density $\varrho(x)$ as the difference δ was allowed to tend to zero.

Acknowledgments

One of us (N.H.M.) wishes to thank Professor J.A. Alonso for generous hospitality during a visit to the University of Valladolid, which enabled this collaborative study. The research of L.M.N has been supported by the Spanish MCYT (BFM2002-03773) and Junta de Castilla y León (VA085/02).

References

[1] A. Holas, N.H. March, *J. Math. Phys.*, **35**, 577 (1994).
[2] N.H. March, *Phys. Rev. A*, **37**, 1869 (1988).
[3] P.A.M. Dirac, *Proc. Roy. Soc. A*, **118**, 351 (1928).
[4] N.H. March, J.C. Stoddart, *Repts. Prog. Physics (UK)*, **31**, Part II, 533 (1968).
[5] E.H. Sondheimer, A.H. Wilson, *Proc. Roy. Soc.*, **A210**, 173 (1951).
[6] J.R. Hiller, *Am. J. Phys.*, **70**, 522 (2002).
[7] C.F. von Weizsäcker, *Z. Phys.*, **96**, 431 (1935).
[8] M.S. Vallarta, N. Rosen, *Phys. Rev.*, **41**, 708 (1932). See also N.H. March, *Electron Density Theory of Atoms and Molecules*, p. 172, Academic Press, New York (1992).
[9] I.A. Howard, N.H. March, *J. Phys. A: Math. Gen.*, **37**, 965 (2004).
[10] G.P. Lawes, N.H. March, *J. Chem. Phys.*, **71**, 1007 (1979).

Appendix: Toward a differential equation for the non-relativistic ground state density $\varrho(x)$ in a linear potential $V = g|x|$

In an earlier work, Lawes and March [10] gave a differential equation for the fermion particle density for one-dimensional harmonic confinement with $V(x) = 1/2x^2$ as

$$\frac{1}{8}\varrho'''(x) + \frac{1}{2}\varrho(x)V'(x) + [N - V(x)]\varrho'(x) = 0 \tag{A1}$$

$N = 1$ corresponding to the lowest state.

The aim of this Appendix is to set out some limiting properties, which a corresponding differential equation for the linear potential $V = g|x|$, though not presently available for general N, must embody.

First, we write the Thomas–Fermi non-relativistic density $\varrho^{\mathrm{TF}}(x)$ in terms of the chemical potential μ as

$$\varrho^{\mathrm{TF}}(x) = K\sqrt{\mu - V(x)} \tag{A2}$$

and find the derivative as

$$\varrho^{\mathrm{TF}\prime}(x) = -\frac{K}{2}\frac{V'(x)}{\sqrt{\mu - V(x)}} \tag{A3}$$

Multiplying both sides of equation (A3) by $[\mu - V(x)]$ and again using equation (A2), we readily obtain

$$[\mu - V(x)]\varrho^{\mathrm{TF}\prime}(x) = -\frac{1}{2}\,\varrho^{\mathrm{TF}}(x)\,V'(x) \tag{A4}$$

This result (equation (A4)) is valid for the limit of large N for a general one-dimensional potential $V(x)$, provided $\mu(N)$ is calculated from equation (A2) to yield $\int \varrho^{\mathrm{TF}}(x)\,dx = N$.

It is already interesting to compare the general result for large N given in equation (A4) with the specific, but exact, result in equation (A1) for harmonic confinement. If one neglects the highest (third) derivative in equation (A1), and then calculates μ from equation (A2) from the normalization condition on $\varrho^{\mathrm{TF}}(x)$ stated above, one finds $\mu = N$ and equations (A4) and (A1) are in accord for large N.

For the lowest state only of the linear potential $V = g|x|$, with eigenvalue ϵ_1, shown in table 1 of the main text, one can, by the use of the properties of the Airy function, or otherwise, readily verify that the particle density $\varrho_1(x) = \psi_1(x)\psi_1^*(x)$ satisfies the linear third-order differential equation

$$\frac{1}{8}\varrho'''(x) + [\epsilon_1 - g|x|]\varrho'(x) - \frac{1}{2}\varrho(x)V'(x) = 0 \tag{A5}$$

However, comparison of equation (A5) with the limiting large N form in equation (A4) above shows that the equation (A5) cannot be true for large N and, while it gives one exact limit for $N = 1$ of the sought-after differential equation for $V = g|x|$, it must be crucially modified away from $N = 1$.